Hydration of Hydrophobic Solutes Treated by the Fundamental Measure Approach

G. N. Chuev* and V. F. Sokolov

Institute of Theoretical and Experimental Biophysics, Russian Academy of Sciences, Pushchino, Moscow Region, 142290, Russia

Received: March 10, 2006; In Final Form: June 1, 2006

We have developed a method to calculate the hydration of hydrophobic solutes by the fundamental measure theory. This method allows us to carry out calculations of the density profile and the hydration energy for hydrophobic molecules. An additional benefit of the method is the possibility to calculate interaction forces between solvated nanoparticles. Based on the designed method, we calculate hydration of spherical solutes of various sizes from one angstrom up to several nanometers. We have applied methods to evaluate the free energies, the enthalpies, and the entropies of hydrated rare gases and hydrocarbons. The obtained results are in agreement with available experimental data and simulations.

I. Introduction

Hydrophobic interactions play an important role in stabilization of various biomacromolecular complexes, including nucleic acids, proteins, and lipids, because these complexes contain a large number of nonpolar groups.[1,2] Despite the long history of studies of hydrophobic interactions, the theoretical treatment of the nature of hydrophobic interactions is still incomplete. The main problem of the interactions is a complicated multiscale character of these effects which can reveal as microscopic changes of water structure near small hydrophobic groups, as well as conformations and aggregation of biomacromolecules at mesoscopic scales up to several tens of angstroms.[3] The Monte Carlo (MC) and molecular dynamics (MD) methods are most frequently used for modeling molecular interactions in solutions.[4] However, their application to the problem of hydrophobic interactions of macromolecules demands huge computing expenses, and in some cases, it is essentially limited because of the specified multiscale character of these interactions. New methods based on a statistical treatment have been actively developed in the past decade.[3,5−8] The most suitable method for the specified effects seems to be the density functional theory (DFT).[9,10] The basic purpose of the approach is to construct the free energy functional of the system which depends on density distribution of liquids particles and intermolecular interaction potentials. Within the framework of this approach there are a lot of various models connected with a concrete choice of the density functional.[11−14]

In our opinion, one of the most perspective DFT models for calculation of solvation phenomena is the fundamental measure theory (FMT)[12−16] which determines the free energy functional as the sum of the weighted contributions dependent on geometrical characteristics of fluid particles. It automatically results in definition of the weighted functions which are responsible for the volume and the surface contributions to the solvation energy. This approach is intimately related to the scaled-particle theory (SPT)[17,18] for the homogeneous hard-sphere fluid, and thus one expects that in the uniform limit, it should reproduce the SPT results. The current status of this theory includes various generalizations of the scheme to different interparticle interactions, binary mixtures and polydisperse systems, application to interfaces, wetting, confined geometries, porous media, and dynamical problems as well (see review, ref 15). In this work, we will calculate the radial distribution functions for rare gases and hydrocarbons, and thermodynamic parameters of their hydrophobic solvation on the basis of the modified FMT, which treats the pressure of the liquid system correctly as distinct from the original FMT. In particular, we will determine the size dependence of the solvation energy and calculate interaction forces between two solutes within the limit of low concentration of the dissolved particles. The rest of this paper is organized as follows. The theory is described in Section II, and the obtained results and the concluding remarks are presented in Section III.

II. Fundamental Measure Theory

The DFT is based on the unequivocal dependence between equilibrium density distribution $n_{eq}(\mathbf{r})$ and external potential $u_{ext}(\mathbf{r})$ acting on a system.[19] The free energy of the system $F[n]$ is related with the thermodynamic (Ω) and the chemical (μ) potentials:

$$\tilde{\Omega}[n, u] = F[n] - \int d\mathbf{r} n(\mathbf{r}) u(\mathbf{r}) \tag{1}$$

where $u(\mathbf{r}) = \mu - u_{ext}(\mathbf{r})$. The equilibrium density $n_{eq}(\mathbf{r})$ is determined by the minimum $\Omega[u] = \tilde{\Omega}[\rho_b, u]$ for the given temperature T:

$$\left.\frac{\delta\tilde{\Omega}[n, u]}{\delta n(\mathbf{r})}\right|_{n_{eq}(\mathbf{r})} = 0, \left.\frac{\delta F[n]}{\delta n(\mathbf{r})}\right|_{n_{eq}(\mathbf{r})} = u(\mathbf{r}) \tag{2}$$

In turn chemical potential μ is determined from boundary conditions, i.e., the equilibrium density should tend to the average density of homogeneous liquid $n_{eq}(\mathbf{r} \to \infty)f\rho_b$. Thus, having the information about functional $\tilde{\Omega}[n, u]$ and the method for evaluation of $n(\mathbf{r})$, we can calculate all necessary equilibrium characteristics of the system. The density functional theory[9] solves the problem by searching the free energy $F[n]$, which consists of two contributions: the ideal ($F_{id}[n]$) and the excess

* Corresponding author phone: 4967 739109; fax: 4967 330553; e-mail: genchuev@rambler.ru.

10.1021/jp061491y CCC: $33.50
Published on Web 08/26/2006

($F_{ex}[n]$) free energies:

$$F[n] = F_{id}[n] + F_{ex}[n], \quad \beta F_{id}[n] = \int n(\mathbf{r})\ln[n(\mathbf{r})\Lambda^3 - 1]d\mathbf{r} \tag{3}$$

where Λ is the de Broglie wavelength, and $\beta = (k_B T)^{-1}$ is the inverse temperature. This free energy is related with the grand canonical functional, minimization of the functional leads to the equilibrium density:

$$n_{eq}(\mathbf{r}) = \rho_b \exp\left[-\beta u_{ext}(\mathbf{r}) + \frac{\delta F_{ex}[n]}{\delta n(\mathbf{r})} - \frac{\delta F_{ex}[n=\rho_b]}{\delta n(\mathbf{r})}\right] \tag{4}$$

Thus, if the functional $F_{ex}[n]$ is known, we can calculate the density profile $n(\mathbf{r})$, and then all required characteristics of the solvation.

There are many ways for constructing $F_{ex}[n]$, most of them use the data on functional derivatives $\partial F_{ex}/\partial n(\mathbf{r})$ and $\partial^2 F_{ex}/\partial n(\mathbf{r})\partial n(\mathbf{r}')$. For Lennard-Jones (LJ) fluids, the excess free energy is decomposed into the contribution from a reference system of hard spheres, and the free energy due to attractive interactions.

$$F_{ex}[n] = F_{hs}[n] + F_{att}[n] \tag{5}$$

The attractive interactions are usually treated by the first-order or the second-order perturbation theories.[20,21] In the mean field approximation, the attraction potential, $u_{att}(r)$, is considered as a perturbation which gives the contribution to the free energy.

$$F_{att}[n] = \frac{1}{2}\int\int [n(\mathbf{r}) - \rho_b] u_{att}(\mathbf{r}-\mathbf{r}')[n(\mathbf{r}') - \rho_b] d\mathbf{r}' d\mathbf{r} \tag{6}$$

Various functionals for inhomogeneous hard-sphere (HS) fluids have been developed. One of such methods is the FMT[12−16] in which the excess free energy is calculated by the use of coarse-grained or smoothed densities. We note that originally this method has been formulated for HS liquids. But later, this method has been applied to spheroids of rotation[22] and also for various repulsive and attractive potentials.[23−25] In HS liquids, the repulsive contribution to the excess free energy is written as follows:

$$\beta F_{hs}[n] = \int \Phi[n_i(\mathbf{r})] d\mathbf{r} \tag{7}$$

where variables $n_i(\mathbf{r})$ are determined as weights

$$n_i(\mathbf{r}) = \int d\mathbf{r}'\, n(\mathbf{r}')\, w^{(i)}(\mathbf{r} - \mathbf{r}') \tag{8}$$

of the density $n(\mathbf{r}')$ averaged with weight factors $w^{(i)}(\mathbf{r} - \mathbf{r}')$ depending on the fundamental geometrical measures of fluid particles, such as volume, surface, etc. The original Rosenfeld formulation[12,13] utilizes the following weighting functions:

$$w^{(3)}(r) = \Theta(\sigma/2 - r),\ w^{(2)}(r) = \delta(\sigma/2 - r),$$
$$w^{(1)}(r) = w^{(2)}(r)/(2\pi\sigma) \tag{9}$$

$$w^{(0)}(r) = w^{(2)}(r)/(\pi\sigma^2),\ \mathbf{w}^{(v_2)}(r) = \delta(\sigma/2 - r)\frac{\mathbf{r}}{r},$$
$$\mathbf{w}^{(v_2)}(r) = \mathbf{w}^{(v_2)}(r)/(2\pi\sigma)$$

where $\delta(r)$ and $\Theta(r)$ are the Dirac delta-function and the Heaviside function, respectively, σ is the diameter of a solvent particle. These weight factors determine weighted densities $n_0(\mathbf{r})$, $n_{v1}(\mathbf{r})$, $n_3(\mathbf{r})$, and the latter is the local factor of packing.

Within the FMT framework,[12−16] the function $\Phi[n_i]$ is determined through six weight densities $n_i(\mathbf{r})$:

$$\Phi[n_i] = -n_0\ln(1 - n_3) + \frac{n_1 n_2 - \mathbf{n}_{v1}\cdot\mathbf{n}_{v2}}{1-n_3} + \frac{n_2^3 - 3n_2\mathbf{n}_{v2}\cdot\mathbf{n}_{v2}}{24\pi(1-n_3)^2} \tag{10}$$

Using these equations and eq 4, we obtain the equilibrium density:

$$n_{eq}(\mathbf{r}) = \rho_b \exp\left[-\beta u_{ext}(\mathbf{r}) + \sum_i \left(\int \frac{\delta\Phi(\mathbf{r}')}{\delta n_i(\mathbf{r}')} w_i(\mathbf{r}-\mathbf{r}')d\mathbf{r}' - \frac{\delta F_{hs}[n=\rho_b]}{\delta n_i}\right)\right] \tag{11}$$

Although the original FMT and the SPT is restricted by the HS fluids, there are no limitations for solute−solvent potential $u_{ext}(r)$. Hence, we may apply the FMT to treat the LJ solutes. The information on the weighted densities also allows us to calculate the mean force potential $W(r)$ determining the interaction force between two solutes in an infinitely diluted solution:

$$W(\mathbf{r}) = V_{uu}(\mathbf{r}) - \sum_i \left(\int \frac{\delta\Phi(\mathbf{r}')}{\delta n_i(\mathbf{r}')} w_i(\mathbf{r}-\mathbf{r}')d\mathbf{r}' - \frac{\delta F_{hs}[n=\rho_b]}{\delta n_i}\right) \tag{12}$$

where $V_{uu}(\mathbf{r})$ is the direct intermolecular interaction potential. In turn, the excess part of thermodynamic potential Ω_{ex} determining the solvation energy is calculated as follows:

$$\Omega_{ex} = \Delta\mu_{ex} = F_{ex} - \sum_i n_i \frac{\delta F_{ex}}{\delta n_i} \tag{13}$$

Since experiments are most commonly done at fixed pressure p, it is convenient to introduce the decomposition of the hydration chemical potential into the excess solvation entropy ΔS and the excess solvation enthalpy ΔH achieved by the use of an isobaric temperature derivative,[26]

$$\Delta S = \left(\frac{\delta\Delta\mu_{ex}}{\delta T}\right)_p,\ \Delta H = \Delta\mu_{ex} + T\Delta S \tag{14}$$

III. Results and Discussion

A. Application to Bulk Water. The FMT reduces to the SPT in the limiting case of homogeneous liquid, determining the pressure p and the surface tension γ_∞ of the liquid at a planar wall[27,28] as

$$\beta p_{hs} = \frac{\delta\Phi(\mathbf{r}\to\infty)}{\delta n_3},\ \beta\gamma_\infty = \frac{\delta\Phi(\mathbf{r}\to\infty)}{\delta n_2} \tag{15}$$

It provides analytical expressions for pressure p and surface tension γ_∞:[27,28]

$$\beta p_{hs} = \frac{n_b[1+\eta+\eta^2]}{(1-\eta)^3},\ \beta\gamma_\infty = \frac{3\eta[2+\eta]}{2\pi\sigma^2(1-\eta)^2} \tag{16}$$

where $\eta = \pi n_b\sigma^3/6$ is the packing factor. In the general case, the pressure p_{hs} is too high to describe water under normal conditions, for example, it yields 8000 atm for the effective HS diameter $\sigma = \sigma_w = 2.77$ Å, corresponding to water at

25 °C.[29,30] Although the attractive contribution (eq 6) decreases pressure p slightly, it cannot provide realistic estimate, since it is considered as perturbation for hard-sphere contribution. On the other hand, eq 15 underestimates the surface tension γ_∞ with respect to the experimental values.

The main origin of these drawbacks is that the behavior of water deviates strongly from that of HS solvent. To exclude these drawbacks, both the thermodynamic parameters are considered as the fitting ones in the modified SPT models (see, for example, refs 31,32). Thus we are to modify the FMT to obtain the realistic estimate for the surface tension. For this purpose, we note that the excess free energy (eq 7) and the solvation energy (eq 13) include volume integral $4\pi[\int_{r_{cut}=0}^{\infty} \Phi[n_i(\mathbf{r})]r^2dr$, while solvation energy $\Delta\mu_{ex}$ also contains the contributions $4\pi \int_{r_{cut}=0}^{\infty} (\delta\Phi(\mathbf{r} \rightarrow \infty)/\delta n_3)\,[n_3(\mathbf{r} \rightarrow \infty) - n_3(\mathbf{r})]r^2dr$ and $4\pi\int_{r_{cut}=0}^{\infty} (\delta\Phi(\mathbf{r} \rightarrow \infty)/\delta n_2)\,[n_2(\mathbf{r} \rightarrow \infty) - n_2(\mathbf{r})]r^2dr$, determined the dependence of solvation energy on the solute radius. We can fit the pressure p and the surface tension γ_∞ by manipulating the cutoff radius r_{cut}, which is zero in the original FMT. Thus, the simplest modification of the FMT method is to exclude small distances $r < r_{cut}$ in eqs 6−8 to decrease the hard-core effect. As a result, the formulas for the thermodynamic parameters are also modified:

$$\beta\hat{p}_{\mathbf{hs}} = \frac{\delta\Phi(r=\infty)}{\delta n_3} - \frac{\delta\Phi(r=r_{cut})}{\delta n_3},$$

$$\beta\hat{\gamma}_\infty = \frac{\delta\Phi(r=\infty)}{\delta n_2} - \frac{\delta\Phi(r=r_{cut})}{\delta n_2} \quad (17)$$

We chose r_{cut} to fit $\hat{\gamma}_\infty$ by the experimental value γ_{exp}. Below, we will indicate that the modified pressure $\hat{p}_{hs}$ also significantly reduces by three orders and plays a minor role in the hydration of hydrophobic solutes. But such modification weakly affects the calculations of the density profile and the excess free energy F_{ex} due to minor contribution of the range $r < r_{cut}$ into integrals $\int\Phi[n_i(\mathbf{r})]d\mathbf{r}$ and $\int d\mathbf{r}'\, n(\mathbf{r}')\, w^{(i)}(\mathbf{r} - \mathbf{r}')$. Of course, our expressions reduce to the conventional formulas for pressure and surface tension[27,28] in the case when $r_{cut} = 0$.

Using the above ad hoc modification of the FMT, we employ the model to evaluate the thermodynamic parameters of bulk water. The HS diameter for water was chosen as $\sigma_w = 2.77$ Å and density of water was $\rho_b\sigma_w^3 = 0.7$. Such choice of the water diameter has been motivated by the solubility experiments of Pierotti.[29] To estimate the attractive contribution (eq 6), we have used the LJ parameters corresponding to the SPC/E model of water.[33] For the solution of eq 11, we used the Picard iterative algorithm. On every k-step of iteration, it was necessary to calculate weight densities $n_i(r)$, which are related with $n_{eq}(r)$ through integrals (eq 8). For improvement of convergence, we used the algorithm based on mixing of parts of the previous and new iterations $n_{in}^k = \lambda n_{in}^k + (1 - \lambda)n_{out}^k$, where λ is the mixing parameter dependent on the bulk density. The step of integration made $0.01\sigma_w$, and the number of points of integration is $N = 2^{12}$. These numerical parameters provide the relative precision of density profiles up to 10^{-6} and for the chemical potential up to 0.1 kcal/mol. Using relations from eq 13 with the cutoff radius, r_{cut}, we have evaluated the excess chemical potential depending on the diameter of the HS solute:

$$\Delta\mu_{ex}(\sigma_u) = \Omega_{ex}(\sigma_u) - \Omega_{ex}(\sigma_u = 0) \quad (18)$$

where σ_u is solute diameter. We used $r_{cut} = 0.42\ \sigma_w$ to fit the calculated surface tension to the experimental value $\gamma_{exp} = 102$ cal/(mole Å^2).[34] Figure 1 represents the dependence of the excess chemical potential $\Delta\mu_{ex}(\sigma_u)/4\pi\sigma_u^2$ obtained by this fitting. Apparently from the figure, our calculations compare very well with the MC results[35] and the calculations received on the basis of the information theory.[36] The figure shows that on the site from 0 up to 4 Å, the curve behaves almost in the linear fashion. It indicates that at such solute sizes, the surface effects do not yield the appreciable contribution to the excess chemical potential, and the volume contribution has crucial importance. Whereas for the particles, whose radius is more than 10 Å, the contribution of the volume component decreases and the surface component grows.

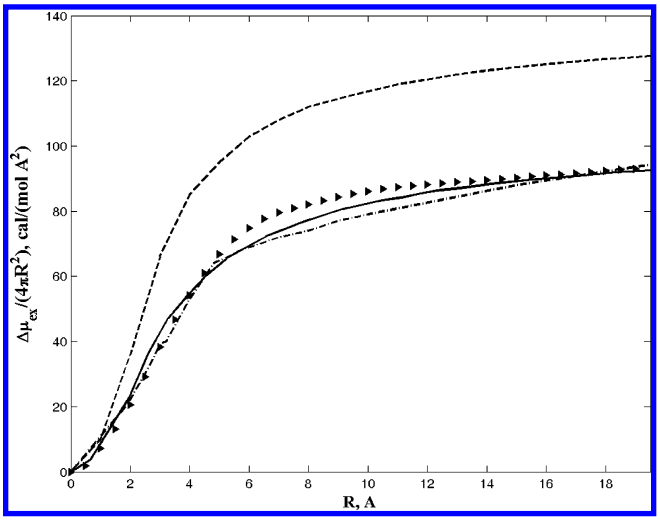

Figure 1. Dependence of the excess chemical potential/surface area of the solute on its HS radius. The solid line is plotted for the modified FMT, the dashed and dash−dotted lines for the modified SPC[31] and the IT,[36] respectively, the triangles correspond to MC simulations (SPC/E water).[35]

We have also calculated the Tolman length δ, which is the surface thermodynamic property of the water vapor−liquid interface (the distance between the equimolar surface and the surface of tension). For this purpose we use the following relation:

$$\Delta\mu_{ex} = 8\pi R^2\gamma_\infty\left(\frac{R-2\delta}{2R-\sigma_w}\right) \quad (19)$$

where $R = \sigma_u/2$ is the solute radius. As a result, we have obtained $\delta = 0.92$ Å which is the MC simulations of the SPC/E water.[35] This value is a little bit more than that calculated in ref 31 ($\delta = 0.9$ Å). But the original FMT provides the following:[27]

$$\delta = \left(\frac{\eta-1}{2+\eta}\right)\frac{\sigma}{2} \quad (20)$$

which is quite different form the experimental data for the SPC water. The pressure of bulk water is estimated as follows:

$$p = \hat{p}_{hs} + \frac{n_b^2}{2}\int u_{att}(\mathbf{r})d\mathbf{r} \quad (21)$$

Table 1 lists the data on the above thermodynamic parameters obtained by the FMT with and without cut of the integration range, as well as the data derived from MC simulations.[35] Although the pressure obtained by our procedure exceeds the simulated one by an order of magnitude, it does not yield the significant effect on the dependence $\Delta\mu_{ex}(\sigma_u)$, since the pressure

TABLE 1: Thermodynamic Parameters of Bulk Water Obtained by the Simulations and by the FMT

	MC [35]	FMT [53]	Modified FMT
$\beta p\sigma_w^3$	5.17×10^{-4}	6.05	4.94×10^{-3}
$\beta\gamma\sigma_w^2$	1.36	1.06	1.32
δ/σ_w	0.32	−0.14	0.33

effect is minor for water under normal conditions. These results hold, however, only at temperatures near 25 °C, since the vapor−liquid interfacial tension of water decreases monotonically with increasing temperature, while the excess chemical potential of hard sphere solutes exhibits a maximum with temperature increasing.

B. HS and LJ Solutes. Based on the designed method, we have carried out calculations for various hydrophobic objects. We have considered the two models of hydrophobic solvation. In the first model, the solute is modeled as hard sphere. In the framework of this model, we have obtained the dependence of the excess chemical potential on the radius of HS solute. Figure 2a shows the comparison of the results received by FMT and by Monte Carlo simulation.[30] The discrepancy between two results are practically missing. The FMT results slightly underestimate the excess chemical potential for hard-sphere solute which has a radius more than 4 Å. To justify our results,

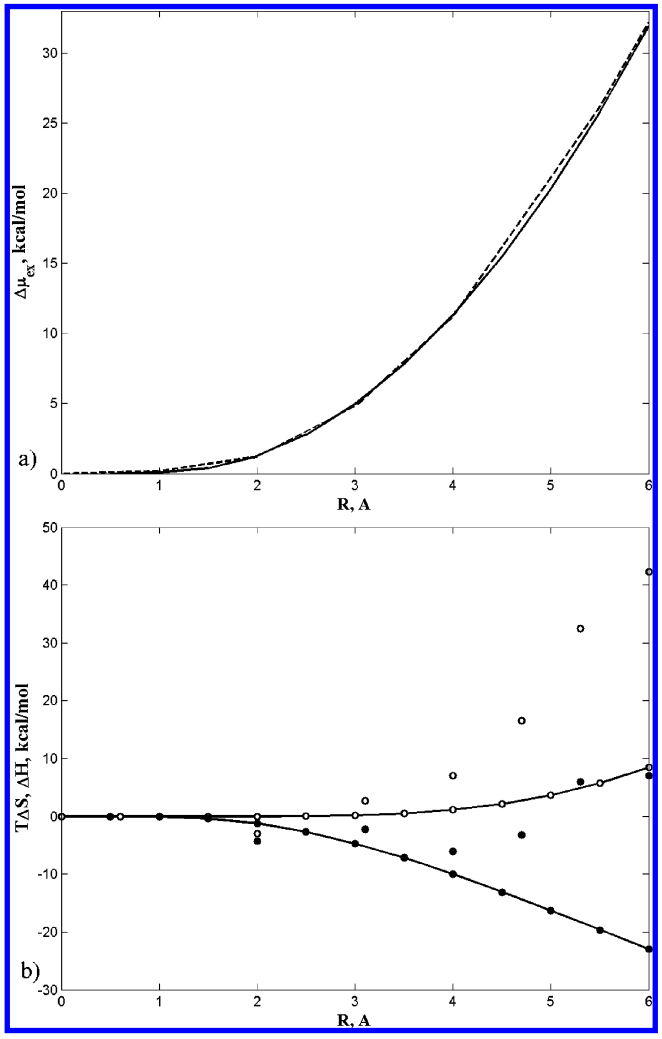

Figure 2. The excess chemical potential, the entropy, and the enthalpy calculated by the MC[30] and by the modified FMT: (a) the excess chemical potential (solid and dashed lines plotted for the FMT and the MC results, respectively), (b) entropies (black circles) and enthalpies (white circles). Symbols with lines and without of them denote the FMT and the MC results, respectively.

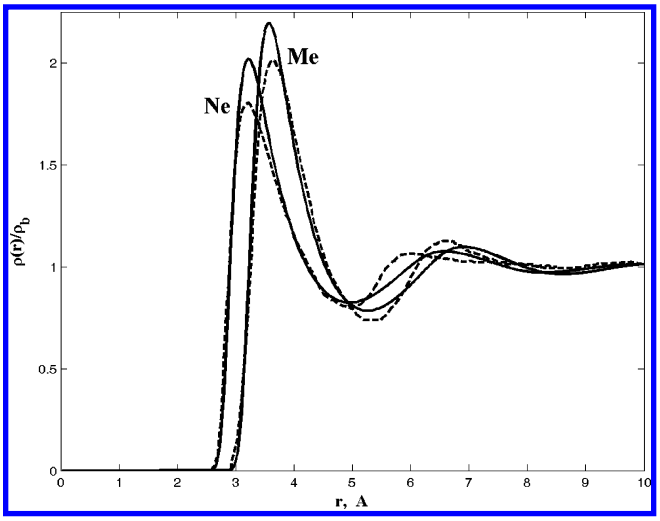

Figure 3. Solute−proximal water oxygen radial distribution functions for neon and methane. The solid line corresponds the modified FMT, while the dashed one to the MD results for Ne[37] and the MC data for Me,[31] respectively.

we have also calculated the enthalpic and entropic contribution into the chemical potential for the HS solute. Figure 2b shows the comparison of the results calculated by the modified FMT with MC results.[30] On one hand, the main difference between the FMT and the MC results is that the FMT as the SPT yields a monotonic decrease of entropy versus the HS diameter, while the MC data indicate more complicated behavior. On the other hand, the magnitude of the excess chemical potential for the HS solutes which radius is a less 6 Å received by MC a slightly exceeds the FMT results.

In the LJ model, the interaction between solute and solvent molecules is realized by the LJ potential

$$u_{\text{ext}}(r) = 4\epsilon\left[\left(\frac{\sigma_{\text{uv}}}{r}\right)^{12} - \left(\frac{\sigma_{\text{uv}}}{r}\right)^{6}\right] \qquad (22)$$

where ϵ_{uv} and σ_{uv} are constructed from the corresponding parameters ϵ_{u}, σ_{u}, ϵ_{v}, and σ_{v} by Lorentz−Berhlot mixing rules. Figure 3 shows the two examples of the radial distribution functions (methane and neon) calculated by the modified FMT and derived from the simulations.[31,37] The discrepancies between the first maxima of the peaks do not exceed 10% and the widths of the peaks are practically coincide. The reason of this difference underlies that the water molecules are modeled as hard spheres and the peaks become higher, and in many instances a bit narrower. Since we have modeled the solutes as spheres, this model seems to be more essential for calculating the excess chemical potential of the atomic solutes. We also will apply this approximation to treat the hydration of hydrocarbons.

C. Inert Gases and Hydrocarbons. For the evidence of the efficiency of the FMT we have calculated radial distribution functions for linear, branched, cyclic hydrocarbons (methane, ethane, butane, etc.), and for rare gases in water. The LJ parameters are presented in Table 2. Based on the HS model we have calculated radial distribution function and evaluated the excess chemical potential for the hydrocarbons and rare gases. The calculation of the excess chemical potential has been carried out with the use of the perturbation theory (PT) to take into account the attractive contribution of the solute−solvent interactions. In this case we have calculated it by using eq 6. The attractive solute−solvent contribution to the hydration free

TABLE 2: Leonard-Jones Parameters of Rare Gases and Hydrocarbons,[39,40] the Experimental[41,52] and Calculated Data on the Excess Chemical Potential, the Enthalpies, and the Entropies of their Hydration

			$\Delta\mu_{ex}$, kcal/mol			$-\Delta H$, kcal/mol			$-T\Delta S$, kcal/mol		
molecule	σ_u, Å	ϵ_u/k_B	exp	LJPT	LJ	exp	LJPT	LJ	exp	LJPT	LJ
helium	2.63	6.03	2.75	3.00	2.76	−	0.49	0.16	−	3.48	2.91
neon	2.79	35.7	2.67	2.62	2.62	0.35	1.23	0.91	3.02	3.84	3.53
argon	3.41	125	2.00	2.21	1.91	2.38	3.09	2.99	4.38	5.30	4.89
krypton	3.67	169	1.66	1.98	1.54	3.20	4.05	4.12	4.86	6.04	5.67
xenon	3.96	217	1.33	1.60	1.38	3.85	5.22	5.40	5.18	6.83	6.79
methane	3.70	157	2.01	2.07	2.11	2.70	3.97	1.70	4.71	6.04	3.80
ethane	4.38	236	1.84	1.61	1.69	3.90	6.55	4.41	5.74	8.20	6.10
propane	5.06	236	1.96	1.67	2.18	4.50	8.70	5.76	6.46	10.50	7.94
butane	5.65	236	2.08	1.45	2.09	6.00	10.93	7.42	8.08	12.64	9.51
pentane	6.16	236	2.33	1.33	2.46	6.25	13.21	8.81	8.58	14.97	11.28
hexane	6.51	236	2.49	3.28	2.55	7.00	12.63	6.11	9.49	16.47	8.66
isobutane	5.55	236	2.24	1.62	2.22	4.95	10.54	7.06	7.19	12.41	9.29
2−methylbutane	5.84	236	2.44	3.33	2.67	−	9.89	4.69	−	13.55	7.36
neopentane	5.89	236	2.51	3.35	2.11	6.10	10.09	5.07	8.61	13.78	7.17
cyclopentane	5.86	236	1.21	1.40	2.03	−	11.82	8.06	−	13.55	10.09
cyclohexane	6.18	236	1.25	1.26	2.01	7.45	13.29	9.10	8.70	14.97	11.12

energy has been estimated as follows:

$$F_{uv} = \rho_b \int g_{hs}(\mathbf{r}) U_{att}(r) d\mathbf{r} \quad (23)$$

where $g_{hs}(\mathbf{r})$ is correlation function of water molecules around the HS solute.[38] For this contribution we have used the Weeks−Chandler−Anderson decomposition for the LJ potential into the attractive and the repulsive parts:[20]

$$u_{att}(r < 2^{1/6}\sigma_{uv}) = -\epsilon,$$
$$u_{att}(r \geq 2^{1/6}\sigma_{uv}) = 4\epsilon_{uv}\left[\left(\frac{\sigma_{uv}}{r}\right)^{12} - \left(\frac{\sigma_{uv}}{r}\right)^{6}\right] \quad (24)$$

where σ_{uv} and ϵ_{uv} are the LJ diameter and well depth, respectively. We denote this approximation as the LJPT model.

Note that the attractive contribution of solvent−solvent interactions energy decreases from 15 to 1% with increasing the solute radius from 0.5 to 20 Å. Opposite, the attractive part of solute−solvent energy increase with increasing the solute radius. Its magnitude is about 80% of the excess chemical potential. Table 2 shows the calculated values of the excess chemical potential, the enthalpies and the entropies for hydrocarbons. The magnitude of the excess chemical potentials for small hydrocarbons (methane, ethane, and propane) is hardly different from experimental results. But the difference of the excess chemical potentials for large solutes becomes more significant. The main reason of it consist in that the solute−solvent attractive contribution for large solutes are essential and it's necessary to know the realistic value of ϵ_u. Since hydrocarbons are molecular solutes, we unfortunately, cannot apply an unique LJ parameter ϵ_{uv} correctly. In much the same way we have calculated the excess chemical potential for rare gases (He, Ne, Ar, Kr, and Xe). At first, we have calculated the energy of cavity formation and two corrections which take into account attractive contributions to the solute−solvent and solvent−solvent interactions. Figure 4 shows the insignificant difference between the experimental values of the excess chemical potential and received by the modified FMT. The agreement between the experimental and the calculated data is strongly quantitative. Table 2 shows that the excess chemical potential with corrections of attractive contributions of the solvent−solute and solvent−solvent energy depends on solute radius in the "U" form.[39] The left and right parts of sign "U" put together the rare gases and the hydrocarbons, respectively.

We have also applied the LJ model and utilized the Lennard-Jones potential for solute−solvent interactions. The discrepancy between the experimental and the calculated values of the excess chemical potential for the rare gases and hydrocarbons is practically missing. Table 2 shows the LJ parameters of the rare gases and hydrocarbons and the results of the calculations. We have carried out the analysis of decomposition the excess chemical potential for hydrocarbons and rare gases on entropic and enthalpic parts. Using eq 14, we have derived the excess chemical potential to two parts ΔH and $-T\Delta S$. Table 2 lists the data on the calculated and the experimental excess chemical potential, the enthalpies, and the entropies of hydration of the hydrocarbons from methane to hexane, the branched hydrocarbons (2-methylpropane, 2-methylbutane, and neopentane), and the cyclic hydrocarbons (cyclopentane and cyclohexane). The FMT calculations by the LJPT and the LJ models are labeled as LJPT and LJ, respectively. We note, similarly,[40] that the obvious feature of the entropic and enthalpic terms is that they are much larger in absolute value than the excess chemical potential. The hydration enthalpies are large and auspicious, and the hydration entropies are large and unfavorable. The entropic terms are marginally larger in absolute value than the enthalpic terms resulting in the unfavorable but small hydration free energies of the hydrocarbons. It is recognized that this behavior

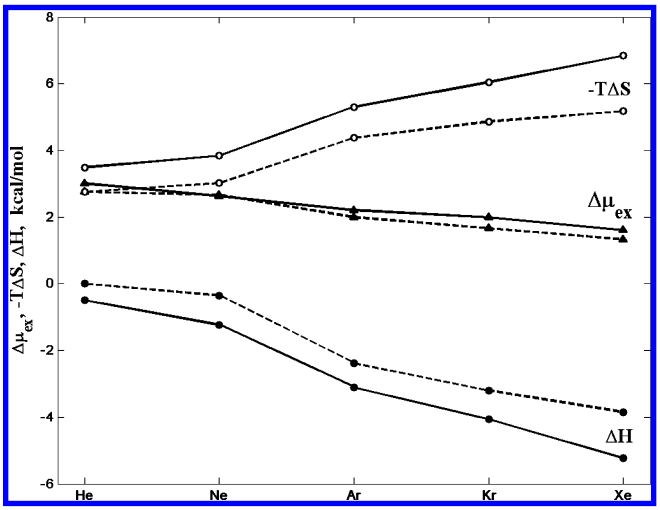

Figure 4. The calculated and the experimental[52] (solid and dashed lines, respectively) data on the excess chemical potentials (triangles), the enthalpies (black circles) and the entropies (white circles) for the rare gases.

is typical of hydrophobic hydration. Solvation of apolar compounds in most other solvents, in fact, is usually accompanied by smaller enthalpic and entropic changes. Table 2 indicates the difference between the experimental[41] and the calculated enthalpies and entropies. The discrepancy in enthalpy does not exceed the 7 kcal/mol for all hydrocarbons. The calculated excess chemical potential of methane is about of 3% more positive than the experimental value (2.01 kcal/mol). The discrepancy between the experimental and calculated hydration enthalpies for normal hydrocarbons is less significant then the similar quantity for the higher hydrocarbons. The difference in the enthalpy and the entropy partially cancels each other resulting in a smaller discrepancy in the excess chemical potential. The calculated and experimental hydration free energies of the hydrocarbons are positive and practically do not increase with solute size.

The fact that the excess chemical potential of ethane is less than methane is well reproduced by our calculations. The modified FMT overestimates the value of enthalpy change and too highly underestimate entropy loss for molecules from methane up to ethane.Both effects bring in less favorable hydration free energy of ethane. It appears, because the current model of hydrocarbons should take into account a larger benefit in favorable hydrocarbon−water interactions in going from methane up to ethane without the further loss of entropy. The hydration enthalpies of the normal and linear hydrocarbons have a tend to increase as solute size rises. The calculations reproduce qualitatively the effect for the LJPT model. The theory overestimates the magnitude of the hydration enthalpies. Fortunately, the difference between calculated and the experimental results are rather closer for the LJ model. The analogue behavior is seen for hydration entropies.

Similarly such decomposition the excess chemical potential into entropic and enthalpic part has been carried out for rare gases. Table 2 shows the discrepancy of solvation free energy for all rare gases to be negligible. The difference between the calculated and the experimental excess chemical potential for all atoms does not exceed 0.33 kcal/mol at temperature 298 K. The calculated solvation entropy are not so close to the experimental value, unlike the calculations of the solvation enthalpy, which overestimates the contribution of it to solvation free energy to a lessor extent. The theory underestimates the values of solvation enthalpy and overestimates the solvation entropy for all rare gases.

The hydrophobic effect is frequently connected to characteristic temperature dependences.[42,43] One of the most surprising observations is the entropy of transition convergence of nonpolar molecules from gas phase or nonpolar solvent into water at temperature about 400 K. We have made the calculations to show that the FMT is able to predict the temperature convergence of entropy both qualitatively, and quantitatively correctly. The calculations have been carried out at several temperatures along the experimental saturation curve of water. Using eq 14 we have obtained the solvation entropy by taking the derivative of the chemical potential along the saturation curve. Figure 5 shows the temperature dependence of the entropy for the different solutes for two cases of calculation. In the first case (Figure 5a), we calculated the excess chemical potential without the fact that the diameter of water decreases with temperature increasing. The entropies are large and negative at room temperature for all the solutes and decrease in magnitude with increasing temperature. The temperature dependence of entropies is approximately linear with slopes increasing with the increasing solute size. Moreover, the entropies converge at about 400 K

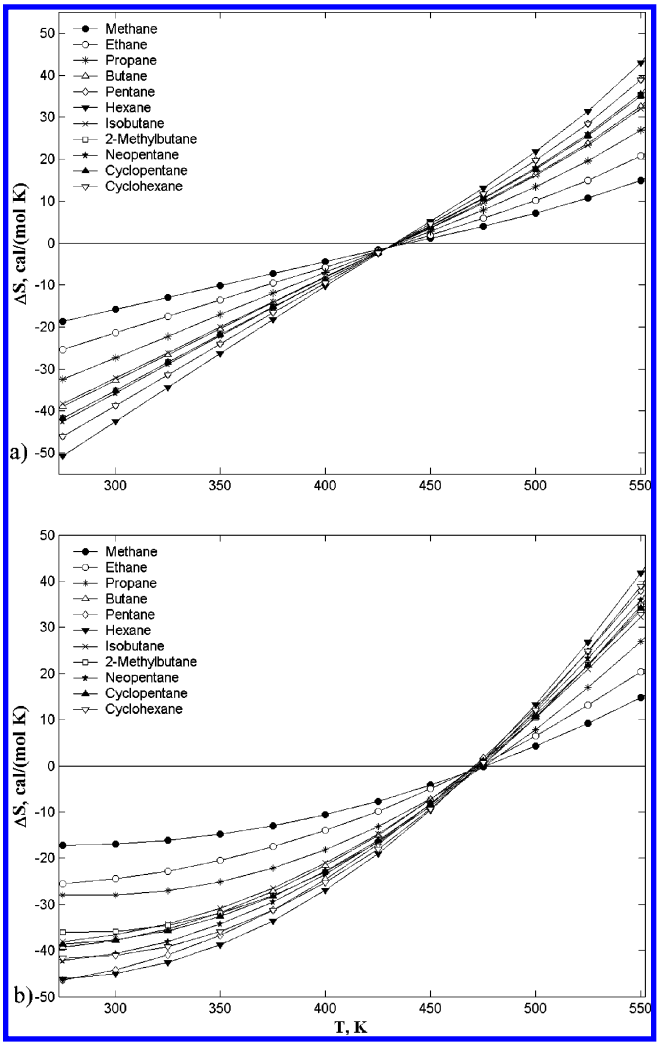

Figure 5. Hydration entropy of HS solutes with radii corresponding hydrocarbons (see legend) as a function of temperature along the saturation curve of water in the case when the water diameter is independent of temperature (a), and temperature dependent (b) like as in ref 44.

to approximately zero entropy, although at closer inspection, the temperature range of the convergence region is several 10 K and the entropy is not exactly zero at convergence. In the second case, we have taken into account the dependence solvent diameter on temperature.[44] Figure 5b shows that the point of entropy convergence has shifted to region where temperature and entropy magnitude is about 470 K and −2.5 cal/(mol K), correspondingly. The convergence region has become a bit wider. It is significant that taking into account the contributions, solute−solvent interactions have changed both the point of entropy convergence (about 500 K) and the width of the convergence region.

D. The Mean Force Potential for Colloids. We have to note the one more benefit of the FMT. The theory allows us to calculate the depletion forces between two the solutes surrounded solvent particles. For macroscopic objects, there are relations for calculation of depletion force for large solutes, depending on the distance between them. The solutes are located in environment of small solvent particles. Viewing hard spheres, Bradley and Hamaker have received the relations which take into account the pair interactions between macroparticles solvated in a simple fluid. Following this approach, the depletion potential W and the depletion force F between two macro-

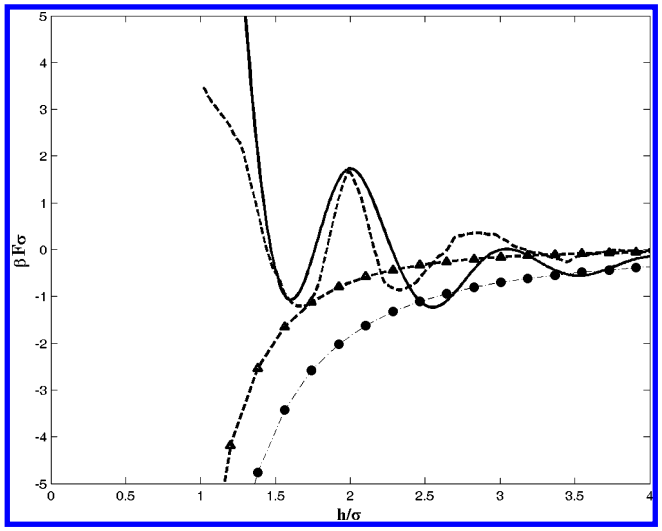

Figure 6. Dependence of the depletion force on the distance between two solutes with radii $R_u = 8.35$ Å and $\beta\epsilon_{uv} = 5$, $\beta\epsilon_v$=1, $\sigma_v = 3.2$ Å. The solid line corresponds to the FMT results, the dashed one to the MD simulations,[46] while triangles and circles to the calculations by the Hamaker and the Bradley formulas.

particles have been calculated depending on the distance h between the solutes:[45]

$$F_B(h) = -\frac{4\epsilon\pi^2\rho_b^2}{12h},\ W_B(h) = -\frac{4\epsilon\pi^2\rho_b^2}{12h^2} \qquad (25)$$

$$F_H(h) = -\frac{4\epsilon\pi^2\rho_b^2}{6}\left[\frac{2}{s^2-4} + \frac{2}{s^2} + \ln\left(\frac{s^2-4}{s^2}\right)\right],$$

$$W_H(h) = -\frac{128\epsilon\pi^2\rho_b^2}{3Rs^3(s^2-4)} \qquad (26)$$

where $s = 2R + h/R$. We have calculated the depletion force $F(h)$ on the FMT basis with the use of the correlation functions obtained before. Apparently from Figure 6, the Hamaker and the Bradley approaches badly feature the behavior of depletion forces near to the solute, yielding strongly underestimated values, and not taking into account the oscillating character of it. The Hamaker and the Bradley approaches adequately predict the depletion force values only in asymptotic distances between the dissolved particles. Unlike them, the FMT allows us to take into account attractive interactions between solutes a bit less than one nanometer. We have also compared the results of MD simulations[46] and that obtained by the FMT. Figure 6 shows that the first peak of FMT results is a bit narrower and higher than MD simulation but localization of curves' zeros almost coincides. The reason of narrowing of the peaks seems to be the modeling of water molecules as hard spheres not as particles interacting via Lennard-Jones potential.

IV. Summary

In this work we have used the FMT for the quantitative description of the hydrophobic phenomena on the basis of the density functional theory. As a result, we have received profiles of radial distribution functions for isolated solutes in a hard-sphere fluid interacting with solute by Lennard-Jones potential. Using the distribution function profile, we have constructed the dependence of the excess chemical potential on the radius of the spherical solutes. To fit the properties of bulk water, namely its surface tension, we have modified the FMT by cutting the radius of integration at small distances. The excess chemical potential has been calculated for several systems, i.e., when interaction between the solute and solvent is simulated as the hard sphere or as the Lennard-Jones potential. We also have shown that the obtained distribution functions reproduce with good precision the oscillating behavior of depletion forces for the particles dissolved in fluid. We have applied methods to evaluate the free energies, the enthalpies, and the entropies of hydrated rare gases and hydrocarbons. The obtained results are in agreement with available experimental data and simulations. We conclude that the original FMT which rigorously should be applied to liquids where all the interactions are described by HS repulsive potentials is also relevant for realistic water-solute potentials. However, such success requires the hard sphere water diameter to be used as an adjustable parameter. The recent extensions of the FMT to soft potentials indicate that the soft FMT is capable to predict the solvent structure for soft repulsive and attractive interaction potentials.[47,48] In this case the FMT yields a systematic way to generalize the treatment for hard bodies to soft interactions. Another bottleneck of the current implementation is the spherical shape of solutes, since the realistic applications should treat the three-dimensional solute structure. There are no restrictions to generalize the above approach to the three-dimensional case, the examples of such generalization are presented in refs 49−51; however, such calculations demand special algorithms and more sophisticated computations. Thus, we think that the FMT can provide a promising basis for the accurate study of hydrophobic molecular solutes.

Acknowledgment. We are thankful to Maxim Fedorov and Michail Basilevsky for fruitful discussions. This work was supported by the Russian Foundation of Basic Research.

References and Notes

(1) Tanford, C. *The Hydrophobic Effect Formation of Micelles and Biological Membranes;* Wiley-Interscience: New York, 1973.
(2) Ben-Naim, A. *Hydrophobic Interactions;* Plenum: New York, 1980.
(3) Lum, K.; Chandler, D.; Weeks, J. D.*J. Phys. Chem. B,* **1999**, *103*, 4570.
(4) Frenkel, D.; Smit, B. *Understanding Molecular Simulation: From Algorithms to Applications*, 1st ed.; Academic Press: New York, 1996.
(5) Hummer, G.; Garde, S.; Garcia, A. E.; Pratt, L. R. *Chem. Phys.* **2000**, *258*, 349.
(6) Pratt, L. R.; Pohorille, A. *Chem. Rev.* **2002**, *102*, 2671.
(7) Huang, D. M.; Chandler, D. *J. Phys. Chem. B* **2002**, *106*, 2047.
(8) Alexandrovsky, V. V.; Basilevsky, M. V.; Leontyev, I. V.; Mazo, M. A.; Sulimov, V. B. *J. Phys. Chem. B* **2004**, *108*, 15830.
(9) Evans, R. *Fundamentals of Inhomogeneous Fluid;* Henderson, D., Ed.; Wiley: New York, 1992.
(10) Barrat, J.-L.; Hansen, J.-P. *Basic Concepts for Simple and Complex Liquids;* Cambridge University Press: Cambridge, 2003.
(11) Curtin, W. A.; Ashcroft, W. *Phys. Rev. A* **1985**, *32*, 2909.
(12) Rosenfeld, Y. *Phys. Rev. Lett.* **1989**, *63*, 980.
(13) Rosenfeld, Y.; Schmidt, M.; Lowen, H.; Tarazona, P. *Phys. Rev. E* **1997**, *55*, 4245.
(14) Tarazona, P. *Phys. Rev. A* **1985**, *31*, 2672.
(15) Löwen, H. *J. Phys.: Condens. Matter.* **2002**, *14*, 118979.
(16) Schmidt, M. *J. Phys.: Condens. Matter.* **2003**, *15*, S101.
(17) Reiss, H.; Frisch, H. L.; Lebowitz, J. L. *J. Chem. Phys.* **1959**, *31*, 369.
(18) Helfand, E.; Frisch, H. L.; Lebowitz, J. L. *J. Chem. Phys.* **1961**, *34*, 1037.
(19) Mermin, N. D. *Phys. Rev.* **1965**, *137*, A1441.
(20) Weeks, J. D.; Chandler, D.; Andersen, H. C. *J. Chem. Phys.* **1971**, *54*, 5237.
(21) Barker, J. A.; Henderson, D. *J. Chem. Phys.* **1967**, *47*, 4714.
(22) Rosenfeld, Y. *Phys. Rev. E* **1994**, *50*, R3318.
(23) Schmidt, M. *Phys. Rev. E* **1999**, *62*, 3799.
(24) Sweatman, M. B. *J. Phys.: Condens. Matter.* **2002**, *14*, 11921.
(25) Ravikovitch, P. A.; Vishnyakov, A.; Neimark, A. V. *Phys. Rev. E* **2001**, *64*, 011602.
(26) Yu, H. A.; Karplus, M. *J. Chem. Phys.* **1988**, *92*, 5020.

(27) Bryk, P.; Roth, R.; Mecke, K. R.; Dietrich, S. *Phys. Rev. E* **2003**, *68*, 031602.
(28) Oversteegen, S. M.; Roth, R.; *J. Chem. Phys.* **2005**, *122*, 214502.
(29) Pierotti, R. A. *Chem. Rev.* **1976**, *76*, 717.
(30) Floris, F. M.; Silmi, M.; Tani, A.; Tomasi, J. *J. Chem. Phys.* **1997**, *107*, 6353.
(31) Ashbauch, H. S.; Paulaitis, M. E. *J. Am. Chem. Soc.* **2001**, *123*, 10721.
(32) Tang, K. E. S.; Bloomfield, V. A. *Biophys. J.* **2002**, *79*, 2222.
(33) Berendsen, H. J. C.; Grigera, J. R.; Straatsma, T. P. *J. Phys. Chem.* **1987**, *91*, 6269.
(34) Alejandre, J.; Tildesley, D. J.; Chapela, G. A. *J. Chem. Phys.* **1995**, *102*, 4574.
(35) Huang, D. M.; Geissler, P. L.; Chandler, D. *J. Phys. Chem. B* **2001**, *105*, 6704.
(36) Basilevsky, M. B.; Grigoriev, V. F.; Leontyev, I. V.; Sulimov, V. B. *J. Phys. Chem. A* **2005**, *109*, 6939.
(37) Kovalenko, A.; Hirata, F. *J. Chem. Phys.* **2000**, *105*, 2793.
(38) Pratt, L. R.; Chandler, D. *J. Chem. Phys.* **1980**, *73*, 3434.
(39) Graziano, G. *J. Phys. Chem. B* **2001**, *105*, 2079.
(40) Gallicchio, E.; Kubo, M. M.; Levy, R. M. *J. Phys. Chem. B* **2000**, *104*, 6271.
(41) Cabani, S.; Gianni, P.; Mollica, V.; Lepori, L. *J. Solution Chem.* **1981**, *10*, 563.
(42) Baldwin, R. L. *Proc. Natl. Acad. Sci. U.S.A.* **1986**, *83*, 8069.
(43) Hummer, G.; Garde, S.; Garcia, A. E.; Paulaitis, M. E.; Pratt, L. R. *J. Phys. Chem. B* **1998**, *102*, 10469.
(44) Graziano, G.; Lee, B. *Biophys. Chem.* **2003**, *105*, 241.
(45) Israelachvili, J. N. *Intermolecular and Surface Forces*, 2nd ed.; Academic: New York, 1992.
(46) Qin Y.; Fichthorn, K. A. *J. Chem. Phys.* **2003**, *119*, 9745.
(47) Schmidt, M. *Phys. Rev. E* **1999**, *60*, R691.
(48) Schmidt, M. *Phys. Rev. E* **2000**, *62*, 4976.
(49) Frink, L. J. D.; Salinger, A. G. *J. Comput. Phys.* **2000**, *159*, 407.
(50) Frink, L. J. D.; Salinger, A. G. *J. Comput. Phys.* **2000**, *159*, 425.
(51) Frink, L. J. D.; Salinger, A. G.; Sears, M. P.; Weinhold, J. D.; Frischknecht, A. L. *J. Phys.: Condens. Matter* **2002**, *14*, 12167.
(52) Pierotti, R. A. *J. Phys. Chem.* **1965**, *69*, 281.
(53) Thermodynamic parameters are evaluated by the analytical expressions obtained in 27.